

# Equilibrium Dynamics in the Non-Diffusive Regime of an Entangled Polymer Blend

D. Lumma, M. A. Borthwick, P. Falus, L. B. Lurio, S. G. J. Mochrie  
 Department of Physics and Center for Materials Science and Engineering,  
 Massachusetts Institute of Technology, Cambridge, Massachusetts 02139

## Introduction

Measurements at the most relevant length and time scales of the relaxation of compositional fluctuations in entangled polymer blends have not been possible thus far. A substantial amount of theoretical work on polymer melt and blend dynamics, based on the reptation hypothesis [1,2], provides incentive for such measurements. The technique of x-ray photon correlation spectroscopy (XPCS) [3] has already been employed to study colloidal suspensions [4], probing length scales comparable to polymer radii of gyration and time scales beyond the plateau separating elastic from viscous polymer blend response. XPCS studies on homogeneous blends are far more challenging than those on colloidal systems, primarily since the scattering cross-sections of blends are significantly smaller. We present an XPCS study of the dynamics of compositional fluctuations in a blend of long, monodisperse, highly-entangled chains, investigating for the first time the relaxation of equilibrium fluctuations on length scales smaller than the extent of individual polymer coils. Compared to melts, polymer blends exhibit a higher level of phenomenological complexity, due to the presence of multiple polymer species. Nevertheless, the dynamic random phase approximation (RPA) may be used to deduce collective blend dynamics from single-chain motion, and allows one to predict the intermediate scattering function (ISF) [5–7], which is experimentally accessible via XPCS [3,4].

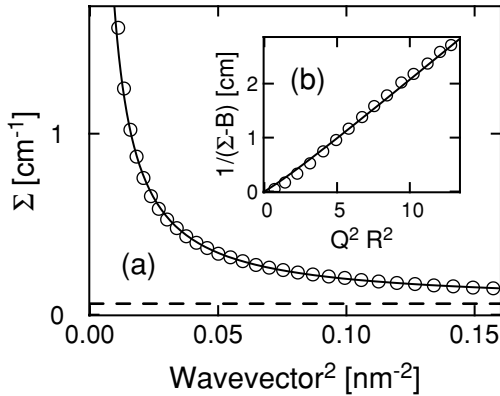


FIG. 1. Static cross-section at 90°C. (a)  $\Sigma$  versus  $Q^2R^2$ . The dashed line indicates the constant background,  $B$ . (b)  $(\Sigma - B)^{-1}$  versus  $Q^2R^2$  for the wavevector range probed dynamically. Solid curves represent a least-squares fit to Eq. 2 for  $0.01 \text{ nm}^{-2} < Q^2 < 0.16 \text{ nm}^{-2}$ .

The reptation model depicts the primary motion of each polymer in such an entangled system as a creep along the length of a tube delimited by temporary entanglements with neighboring chains. XPCS assumes a nonpareil position in probing the viscous regime of entangled blends, allowing for microscopic measurements at time scales of up to tens of seconds or longer. Thus, XPCS enables us to characterize a previ-

ously inaccessible region of dynamic phase space, providing a direct measurement of reptative features in the diffusion of a polymer blend.

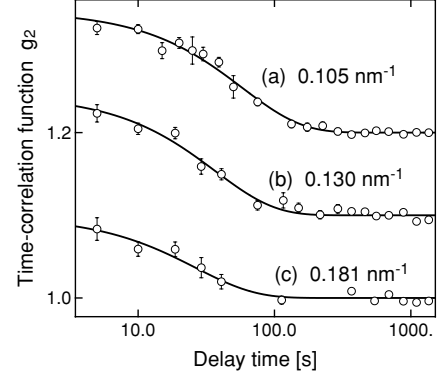


FIG. 2. Measured correlation functions,  $g_2(Q, t)$ , versus delay time,  $t$ , for three different wavevectors at 70°C. The autocorrelation baselines were offset by (a) 0.2 and (b) 0.1.

## Methods and Materials

Symmetric blends of poly(ethylene oxide) ( $M_w = 334.5 \text{ kg/mol}$ ,  $M_w/M_n = 1.14$ ) and poly(methyl methacrylate) ( $M_w = 281.0 \text{ kg/mol}$ ,  $M_w/M_n = 1.06$ ) were prepared by solution casting. We calculate a volume-averaged mean-square radius of gyration of  $R = 18.3 \text{ nm}$ .

The small-angle x-ray scattering setup used for our experiments is described in Ref. [4]. Dynamical properties of the blend were characterized via intensity autocorrelation of sequences of CCD images. The normalized correlation function,  $g_2(Q, t)$ , is related to the ISF,  $f(Q, t) = S(Q, t)/S(Q)$ , via

$$g_2(Q, t) = 1 + A f^2(Q, t), \quad (1)$$

where  $t$  is the delay time, and  $A$  the optical contrast. To determine the contrast independently of the blend, we also performed autocorrelation of the scattering from a static silica aerogel sample [16].

## Results

Shown in Fig. 1(a) is the cross-section per unit sample volume ( $\Sigma$ ) of the blend held at 90°C, fitted to

$$\Sigma = \Delta \rho_e^2 r_e^2 \left\{ \sum_i [\varphi_i v_i N_i P_i(Q^2 R_{g,i}^2)]^{-1} - \frac{2\chi}{v_0} \right\}^{-1} + B. \quad (2)$$

The first term describes compositional fluctuations in a binary blend according to the random phase approximation [13], and the second term ( $B$ ) denotes background scattering. In Fig. 1(b), we show the inverse of the background-subtracted cross-section, i.e.  $(\Sigma - B)^{-1}$ .

Blend correlation functions are shown in Fig. 2. Assuming an exponentially decaying ISF, we performed least-squares

fits to Eq. 1 to determine the decay rate and the apparent contrast at each wavevector. The best fits are shown in Fig. 2. The relaxation rates at 70°C are plotted in Fig. 3. Blend and aerogel contrast are shown in Fig. 4(a).

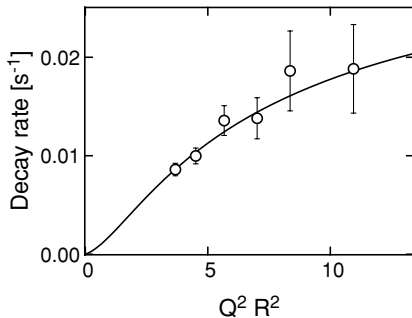


FIG. 3. Relaxation rates at 70°C versus  $Q^2R^2$  (○). The solid curve corresponds to the model described in the text.

### Discussion

Modelling of the ISF by means of the dynamic RPA for a monodisperse, entangled homopolymer blend [7] shows that we should expect the decay rate to vary as illustrated by the solid line in Fig. 3. Using data on the disentanglement times from Ref. [10], we have obtained the curve of Fig. 3 by fitting a single adjustable parameter. The dynamic RPA apparently describes the observed relaxation rates very well.

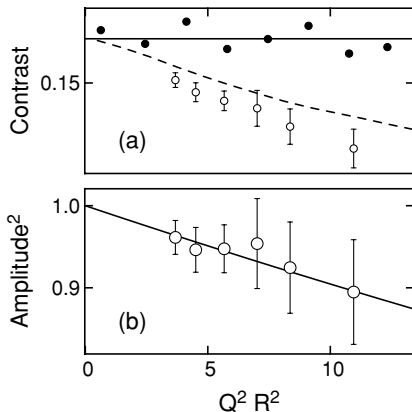


FIG. 4. Observed wavevector dependence of the mode amplitude. (a) Measured contrast of the aerogel (●), and of the blend at 70°C (○), plotted versus  $Q^2R^2$ . The dashed line shows the contrast reduction expected from background scattering, proportional to  $(1-B/\Sigma)^2$ . (b) Ratio of the apparent blend contrast to the contrast accessible for characterizing slow relaxations of compositional fluctuations. The solid curve represents the model described in the text.

A systematic difference between blend and aerogel contrast is evident in Fig. 4(a): while the aerogel contrast exhibits no observable dependence on wavevector, the apparent blend contrast decreases with  $Q^2R^2$ . We interpret this decay as due to the presence of modes faster than can be resolved by our detection scheme. If the static background,  $B$ , is in fact due to a fast dynamic process, such as phonon scattering, the contrast ratio will be reduced by a wavevector-dependent factor,  $(1-B/\Sigma)^2$ , shown in Fig. 4(a) by the dashed line. This contribution is not large enough to account for the entire decrease

of the mode amplitude. In Fig. 4(b), we have corrected the apparent contrast for the effect of the background, yielding the ratio between the contrast actually observed in the blend data to the contrast that should be available for the characterization of dynamic processes with accessible relaxation rates. The resulting data of Fig. 4(b) lie systematically below unity.

Within the reptation model, the mode amplitude of the curvilinear creep in *melts* is predicted to be proportional to  $a_r = \exp(-Q^2d^2/36)$ , where  $d$  is the diameter of the confining tube [9]. The best fit of  $a_r^2$  to the amplitude data yields the solid line in Fig. 4(b), corresponding to a tube diameter of  $d \approx 7.8 \pm 3.4$  nm. From the entanglement molecular weights of the component chains [11,12], we infer their entanglement lengths in the melt as 4.7 nm for PEO and 5.2 nm for PMMA, leading to an expected tube diameter of  $d \approx 5$  nm in the blend. Considering both Figs. 3 and 4, we conclude that the reptation model is successful in providing a quantitative description of our findings.

### Acknowledgements

8-ID was developed with support from the NSF (DMR 9312543), from the DOE (DE-FG02-96ER45593), and from NSERC. Work at MIT was also supported by the NSF (DMR 9808941). The APS is supported by the DOE (W-31-109-Eng-38). We thank Harold Gibson for his expert assistance.

- 
- [1] P. G. de Gennes, *J. Chem. Phys.* **55**, 572 (1971).
  - [2] M. Doi and S. F. Edwards, *J. Chem. Soc. Faraday Trans. II* **74**, 1789 (1978).
  - [3] See, for example, S. G. J. Mochrie, A. M. Mayes, A. R. Sandy, M. Sutton, S. Brauer, G. B. Stephenson, D. L. Abernathy, and G. Grübel, *Phys. Rev. Lett.* **78**, 1275 (1997), as well as references therein.
  - [4] L. B. Lurio, D. Lumma, P. Falus, M. A. Borthwick, S. G. J. Mochrie, J.-F. Pelletier, M. Sutton, A. Malik, and G. B. Stephenson, *Phys. Rev. Lett.* **84**, 785 (2000).
  - [5] P. Pincus, *J. Chem. Phys.* **75**, 1996 (1981).
  - [6] K. Binder, *J. Chem. Phys.* **79**, 6387 (1983).
  - [7] A. N. Semenov, *Physica A* **166**, 263 (1990).
  - [8] P. E. Rouse, *J. Chem. Phys.* **21**, 1272 (1953).
  - [9] P. G. de Gennes, *J. Physique* **42**, 735 (1981).
  - [10] J. A. Zawada, C. M. Ylitalo, G. G. Fuller, R. H. Colby, and T. E. Long, *Macromolecules* **25**, 2896 (1992).
  - [11] S. Wu, *J. Polym. Sci. B: Polym. Phys.* **27**, 723 (1989).
  - [12] K. Fuchs, C. Friedrich, and J. Weese, *Macromolecules* **29**, 5893 (1996).
  - [13] J. S. Higgins and H. C. Benoît, *Polymers and Neutron Scattering* (Clarendon Press, Oxford, 1994).
  - [14] H. Ito, T. P. Russell, and G. D. Wignall, *Macromolecules* **20**, 2213 (1987).
  - [15] J. Kugler, E. W. Fischer, M. Peuscher, and C. D. Eisenbach, *Makromol. Chem.* **184**, 2325 (1983).
  - [16] A. R. Sandy, L. B. Lurio, S. G. J. Mochrie, A. Malik, G. B. Stephenson, J.-F. Pelletier, and M. Sutton, *J. Synchrotron Rad.* **6**, 1174 (1999).